



This is a repository copy of *Tribological behaviour of self-lubricating Mg matrix composites reinforced with silicon carbide and tungsten disulfide*.

White Rose Research Online URL for this paper:
<http://eprints.whiterose.ac.uk/157018/>

Version: Accepted Version

Article:

Zhu, J., Qi, J. orcid.org/0000-0001-5235-0027, Guan, D. et al. (2 more authors) (2020) Tribological behaviour of self-lubricating Mg matrix composites reinforced with silicon carbide and tungsten disulfide. *Tribology International*, 146. ISSN 0301-679X

<https://doi.org/10.1016/j.triboint.2020.106253>

Article available under the terms of the CC-BY-NC-ND licence
(<https://creativecommons.org/licenses/by-nc-nd/4.0/>).

Reuse

This article is distributed under the terms of the Creative Commons Attribution-NonCommercial-NoDerivs (CC BY-NC-ND) licence. This licence only allows you to download this work and share it with others as long as you credit the authors, but you can't change the article in any way or use it commercially. More information and the full terms of the licence here: <https://creativecommons.org/licenses/>

Takedown

If you consider content in White Rose Research Online to be in breach of UK law, please notify us by emailing eprints@whiterose.ac.uk including the URL of the record and the reason for the withdrawal request.



eprints@whiterose.ac.uk
<https://eprints.whiterose.ac.uk/>

Tribological behaviour of self-lubricating Mg matrix composites reinforced with silicon carbide and tungsten disulfide

Juanjuan Zhu^{a*}, Jiahui Qi^b, Dikai Guan^b, Le Ma^c, Rob Dwyer-Joyce^a

^aThe Leonardo Centre for Tribology, Department of Mechanical Engineering, University of Sheffield, Mappin Street, Sheffield, S1 3JD, UK

^bDepartment of Materials Science and Engineering, University of Sheffield, Mappin Street, Sheffield, S1 3JD, UK

^cSorby Centre, Kroto Research Institute, North Campus, University of Sheffield, Broad Lane, Sheffield, S3 7HQ, UK

* Corresponding author: Juanjuan Zhu, E-mail address: juan.zhu@sheffield.ac.uk

Abstract

In this study, magnesium matrix composites reinforced with 5 wt% WS₂ and 15-20 wt% SiC particles were sintered via powder processing. The friction and wear behaviour were studied using a ball-on-disc tribometer against Al₂O₃ ball, subjected to normal loads of 1-4 N, room temperature and 110 °C, sliding speed of 22.5 mm/s, and lubricant of PAO base oil. The wear track and tribo-layer generated were investigated by optical profilometry and scanning electron microscopy. The average friction coefficient for Mg metal matrix composites (MMCs) was found to be 0.1-0.2 compared with 0.16-0.46 for pure Mg. Under all testing conditions, the Mg MMCs exhibited much lower friction coefficient and outstanding anti-wear property compared with unreinforced Mg and the Mg alloy AZ31.

Keywords: magnesium metal matrix composite, tribological behaviour, self-lubricating, friction and wear

1. Introduction

Lightweight metal matrix composites are recently becoming more popular for high efficiency applications, including automobile, aerospace, defence and telecommunication industries. These composites have superior physical and mechanical properties, such as light weight, high specific strength, high specific modulus [1-2]. The improved physical and mechanical properties are achieved by combining lightweight metal/alloy with other additives that are in the form of particles, whiskers or fillers [3-6].

Among common lightweight metals, magnesium (Mg) has the lowest density of 1.74 g/cm³ which is approximately 35% less than that of aluminium (Al) (2.7 g/cm³), 77% less than that of steel (7.9 g/cm³) and comparable to plastics (0.92 - 2.17 g/cm³) [7-8]. In addition, Mg shows better physical properties compared with Al and titanium (Ti), including processing, machining and recycling, which can reduce recurrent costs [9]. The usage of Mg has been constantly increasing according to available literature [10-12].

However, Mg and its alloys are primarily used in structural applications for component weight saving [13]. The main restrictions for use as load bearing and tribological machine elements are their moderate strengths at both room and elevated temperatures as well as poor frictional behaviour. It is well recognized that when a soft metal like Mg slides against hard material without liquid or solid lubrication, the softer one will abrade, or flow and adhere to the hard material, creating an interface of low shear strength. These drawbacks lead to a reduced service time for Mg-based parts and making Mg unsuitable for usage in bearings, gears, pistons and cylinders [14-17].

One solution is to develop Mg MMCs dispersed with reinforcements for improving mechanical and tribological properties. Studies have been carried out on how the incorporation of stiffer

phases such as hard ceramic particles, whiskers or fibres into Mg and Mg based alloys can increase specific strength, specific modulus as well as wear resistance [18-21]. Dieringa reported that micro particles or fibres reinforced Mg alloys exhibit satisfactory creep strengths at temperatures up to 250 °C [22]. A variety of hard particles, such as SiC, Al₂O₃, CaB₆, ZnO, SiO₂ and TiB₂ were investigated as reinforcement [12, 23-30]. Among those stiffer reinforcements, due to their low cost and the possibility of homogeneous distribution in the metal matrix composites, the use of SiC particles as the reinforcement in Mg MMCs has become more favourable [19-20, 31-32]. Shen et al. studied the influence of micro SiC particles on the tensile properties of Mg alloy (AZ31B). It was found that the addition of 5 vol% SiC particles improved the elastic modulus as well as ultimate tensile strength and yield strength [19]. Through spark plasma (SPS) sintering technology, Muhammad et al. [33] studied the influence of SiC particle content in the pure Mg and the Mg alloy AZ31 on the microstructure and mechanical properties of Mg composites. The hardness and tensile strength of Mg MMC was found to be increased with increasing SiC content up to 10 wt%. Landkof [20] found that AZ91 based MMC with up to 30% weight fraction of SiC reinforcement showed significantly improved tensile strength, yield strength and elastic modulus at both room temperature and 150 °C. The strengthening mechanism is that SiC particles constitute obstacles at grain boundaries that prevent boundary sliding. Regarding wear resistance, it is not always improved by increasing SiC portions and a 25 vol% SiC was found to deteriorate the wear resistance of QE22 magnesium alloy [31].

Even though the mechanical properties are enhanced by stiffer additions, there is a downside from the abrasiveness of these hard particles as they cause a high friction coefficient in the contact above a certain carried load [33]. In order to reduce the friction in the lubricating applications, solid self-lubricating agents such as, graphite, WS₂ (platelets of the 2H polytype), MoS₂ are used in the metal matrix to achieve improved lubricating properties. Due to the layered chemical structure, these solid lubricants possess weak inter-layer (van der Waals) bonds which provides minimum tangential resistance and therefore low-strength shearing [34-37].

Compared with MoS₂, WS₂ has been found to be a superior friction modifier as it works in both dry and humid conditions and has a high temperature resistance [34, 38-45]. There are two types of WS₂ based on its chemical structure: 2H (platelets of the 2H polytype) which have a layered structure, and IF (inorganic fullerene structure) where the layers are rounded up to form multi-layered spherical ‘onion-like’ cages [43]. It was found that 2H-WS₂ was more prominent in friction reduction compared with IF-WS₂ in dry sliding contact at 25 °C [43]. Rapoport et al. [34] reported the outstanding tribological performance of 2H-WS₂ hollow nanoparticles operating as solid lubricant through both ball-flat and disc-block experiments. In this study, 2H-WS₂ was studied as an additive and is referred as WS₂ for simplicity.

Although WS₂ presents improvements in friction reduction and wear resistance when added to MMCs, there are challenges existing in the composites preparation as WS₂ tends to react with molten metals at higher temperature [46-48]. There are two manufacturing methods for lightweight MMCs: sintering and casting. The former process is not suitable for scale-up because it is only effective on a small scale. The later approach is to use a technique where the metal is liquefied and other materials are added followed by stir mixing. However, it was reported that under high pressure and temperature, WS₂ tends to react with the metal material [49-50]. In this study, a powder metallurgy process was used for manufacturing self-lubricating MMCs as it requires lower manufacturing temperatures, avoiding the reaction between WS₂ and metal matrix before its operational use [43].

Although 3-5 wt% WS₂ reinforced Al composites have been intensively studied for tribological and mechanical properties [37, 40-43, 51-52], there is no research carried out towards WS₂ reinforced Mg MMCs. In this work, SiC and WS₂ reinforced Mg MMCs were sintered through Spark Plasma Sintering (SPS). Tribological behaviour of Mg MMCs were studied for the first time through ball-on-disc reciprocating tests. The role of SiC and WS₂ in improving Mg MMCs' mechanical strength, reducing friction and wear under reciprocating sliding conditions was investigated.

2. Materials and methods

2.1 Composite metallurgy and testing samples

Mg powder ($\geq 99\%$ purity) with a particle size ranging from 63 to 250 μm (Sigma-Aldrich Inc.) was used as a matrix material. Silicon carbide (SiC) particles with average particle size of 30 μm (Thermo Fisher Scientific Inc.) were used as one reinforcement phase to improve the matrix mechanical strength. Tungsten disulfide with average particle size of 2 μm (Sigma-Aldrich Inc.) were used as the second reinforcement phase for friction and wear reduction. The weight fraction of SiC was 15-20 wt% while the fraction for WS₂ particles was 10 wt%. All composites were consolidated using SPS [53-55]. The manufacturing process involves homogeneously mixing the base matrix material and filler powders using a cryomill (Retsch, Germany), followed by pre-compacting at 10MPa pressure and consolidating at 50MPa and 450 °C by SPS system (FCT Systeme GmbH, type HP D1050, Germany) under vacuum. A cylindrical graphite die with diameter of 20 mm was used for the mixed powder sintering. The temperature was monitored by a thermal couple inserted in a pre-drilled hole located in the middle of the outer wall on the die. A thin graphite foil was placed around the inner surface of the die before filling in mixed powders to avoid welding and obtain a more uniform current flow. A heating rate of 50 °C/min was adopted followed by a dwell time 5 min with a uniaxial pressure of 50 MPa and a holding temperatures of 450 °C. In order to compare with matrix composites, the as-received Mg powder was sintered following the same procedure. In addition, a commercial as-received extruded AZ31 (Luxfer MEL Technologies, Manchester, UK) was tested for comparison.

SPS sintered cylindrical Mg MMCs composite bars had dimensions of approximate 20 mm diameter \times 12 mm long. Round discs with dimensions of 19 mm diameter \times 3.5 mm thick were machined by electrical discharge machining (EDM). Figure 1 shows the sketch of the sintered composites and EDM sliced discs. Table 1 lists the experimental samples in this work. The composite density of the sintered samples was measured using a balance with accuracy of ± 0.0001 g (MS104S, Mettler Toledo, Switzerland) which follows the Archimedes principle. Three measurements were taken for each sample and the average was used. The Vickers hardness was conducted using a Durascan 70 (Struers, United Kingdom) micro-hardness tester on the polished Mg MMC surfaces. A Vickers diamond indenter tip was used with a load of 0.1 N and a hold time of 10 s for each micro-hardness indentation. An array of twenty micro hardness indentions was performed at interval distances of 1 mm for each sample and the average Vickers hardness was used. The elastic modulus was determined using a Bruker Hysitron TI Premier Nanoindenter with a normal load of 10 mN (the indentation depth is about 0.9 μm) and a hold time of 5s for each indentation, while the Poisson's ratio was set at 0.35. For each sample, a matrix of 6 \times 6 nano-indentions was performed at interval distances of 100 μm and the average elastic modulus was adopted. The Oliver and Pharr method was used to analyse the elastic modulus from the nano-indentation data [56-57].

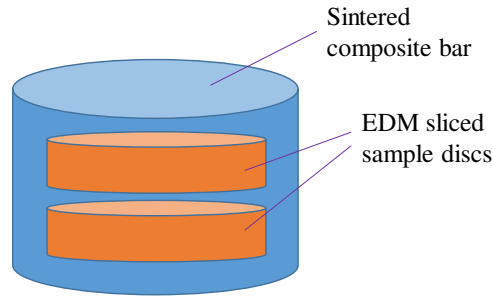


Figure 1. SPS sintered Mg MMC bar and EDM sliced discs

Table 1. Experimental samples used in this work

Sample designation	Materials	fabrication method	Density (g/cm ³)	Relative density, %	Hardness, Vickers	Elastic modulus, GPa
Mg	magnesium	Powder metallurgy, SPS sintered	1.734	100	38.9	36.4
Mg MMC1	75 wt% Mg, 15 wt % SiC, 10 wt% WS ₂	Powder metallurgy, SPS sintered	1.98	97.6	72.8	45.2
Mg MMC2	70 wt% Mg, 20 wt% SiC, 10 wt% WS ₂	Powder metallurgy, SPS sintered	2.01	96.3	80.8	43.7
AZ31	3 wt% Al, 1 wt% Zn, Mg alloy	Extrusion, as received	1.8	-	90	45

The hardness and elastic modulus values are essential for studying a material's tribological performance. As shown in Table 1, the presence of the reinforcement particles in the Mg matrix results in an increase in hardness and the elastic modulus. Mg MMC2 presented slightly lower relative density compared with Mg MMC1. Due to the difference in chemical composition, the bonding between the reinforcement particles and the matrix Mg particles is weaker compared with the bonding between the Mg matrix particles. A decreased relative density is therefore expected with increasing reinforcements. The influence of these reinforcements on the tribological performance of the composite is assessed through friction tests.

2.2 Friction tests

Tribological behaviours of Mg MMC samples were examined using a Bruker Universal Mechanical Tester (UMT) platform under room temperature and 110 °C. The contact configuration was made of Mg MMC composite discs sliding against a static alumina ceramic ball (Al₂O₃, grade 25, 4 mm diameter, elastic modulus 407 GPa, Vickers hardness 1365 Hv, Poisson ratio 0.21). The ball was held in a chuck and loaded against the flat disc which was immersed in oil. New specimens (balls and discs) were used for each test and were cleaned with solvents in an ultrasonic bath prior to the test. The sliding tests were conducted with a polyalphaolefins oil (PAO), which has a density of 832 kg/m³ and a viscosity of 46.73 cSt at 40 °C and 7.96 cSt at 100 °C. Base oils have low polarity affinity for metal surfaces, it is therefore chosen to avoid any competition between the WS₂ particles and the oil molecules for the metal surface [43, 58].

EDM sliced Mg MMC discs were subjected to a standard grinding and polishing process in order to obtain identical surface finishes for the varying samples. SiC paper from 1200 to 4000 grit were used for grinding following by buff polishing with alcohol based diamond suspensions of 1 and 0.25 μm to minimise oxidation through exposure to water.

The reciprocating sliding tests were carried out with a normal load of 1 N and 4 N. Table 2 summaries the testing conditions. Based on the measured mechanical properties of Mg MMCs (Table 1), the corresponding initial mean Hertz pressures were calculated and shown in Table 3.

Table 2. Reciprocating sliding test conditions

Normal load	Stroke distance	Sliding speed	Testing duration	Ball material	Ball diameter	Disc material	Temperature
P = 1, 4 N	4.5 mm	22.5 mm/s (2.5 Hz)	60 min	Al ₂ O ₃	4 mm	Mg MMCs, Mg alloy	Room temperature and 110 °C

Table 3. Initial mean Hertz contact pressures for tested materials corresponding to 1 N and 4 N

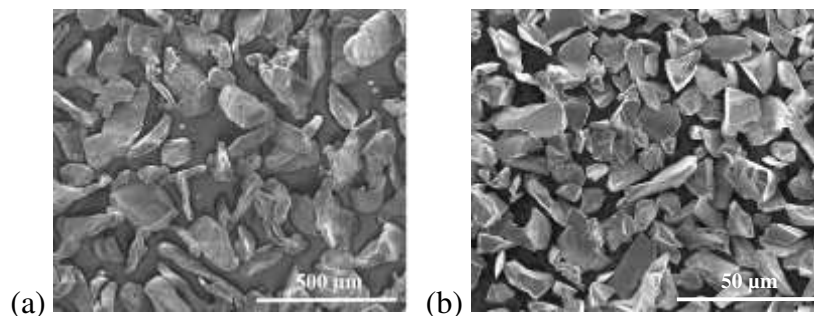
Sample designation	Hertz pressure at P = 1 N, MPa	Hertz pressure at P = 4 N, MPa
Mg	274	435
Mg MMC1	312	495
Mg MMC2	306	485
AZ31	311	494

2.3 Characterisation

In this study, Inspect F FEG scanning electron microscopy (SEM) (FEI, Netherlands) attached with an energy dispersive X-ray (EDX) detector, was used to characterize composite particles, fresh surfaces, worn surfaces and elements distribution on the fresh and tested samples. Wear tracks were assessed using an Alicona InfiniteFocusSL microscope (Alicona Imaging GmbH, Graz, Austria). 3D morphology and depth information from the worn surface was examined using optical microscopy and the focus variation technology of the Alicona. This information was then proceeded for wear scar volume, including dimensions of the wear scar. The size of the wear track and the ball surface were examined after each test with an optical microscope, Zeiss Optical Microscope (Zeiss, United Kingdom).

3. Results and discussion

Figure 2 shows SEM images of as received Mg particles (Figure 2 (a)), SiC particles (Figure 2(b)) and WS₂ particles (Figure 2 (c) and (d)). A lamellar structure of WS₂ particles can be observed with particle size between 1-5 µm.



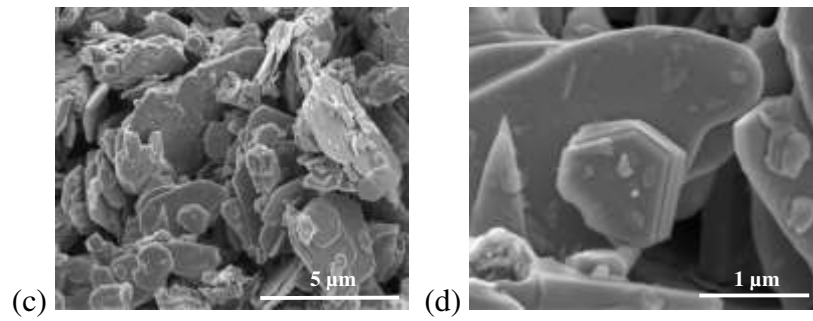


Figure 2. SEM images of (a) Mg particles, (b) SiC particles, (c) and (d) WS₂ particles

Figure 3 shows SEM images of the surface morphology for sintered Mg and Mg MMCs. For the pure Mg sample, particle boundaries can be clearly observed, shown in Figure 3 (a). For Mg MMC1 and MMC2 that followed the same sintering process, Mg particle boundaries were filled with additive powders instead, shown in Figure 3 (b) and (c). The accumulation of SiC and WS₂ particles at the Mg particle boundary were expected to improve the mechanical and self-lubricating properties of Mg MMCs, shown in Figure 3 (d).

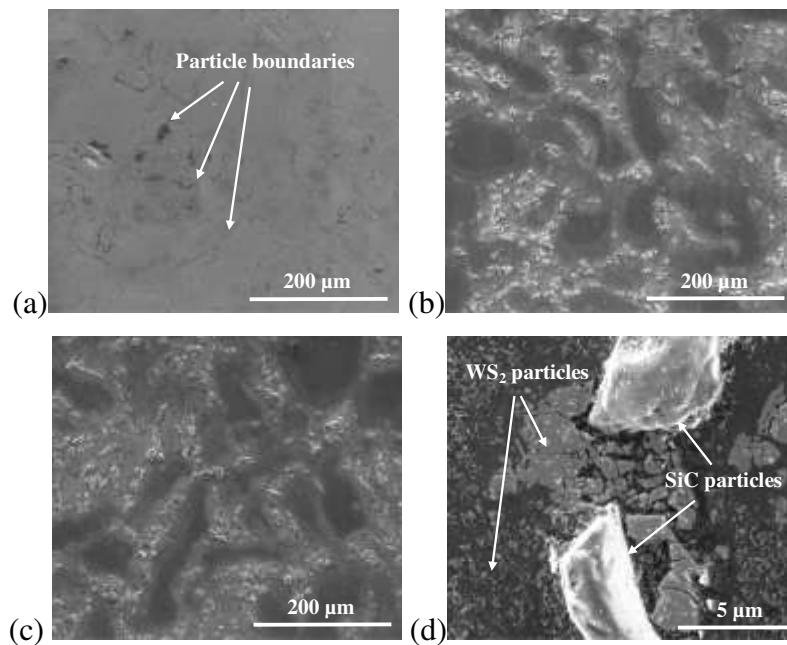


Figure 3. SEM images showing microstructure of Mg MMC composites, (a) Pure Mg, (b) Mg MMC1 (75 wt% Mg, 15 wt% SiC, 10 wt% WS₂), (c) Mg MMC2 (70 wt% Mg, 20 wt% SiC, 10 wt% WS₂), and (d) SiC and WS₂ particles on the Mg particle boundaries on Mg MMC2

Figure 4 shows the evolution of the coefficient of friction (CoF) against reciprocating time between the alumina ball and Mg composites or alloy subjected to varying testing temperatures and normal loads. Under all testing conditions, the presence of WS₂ has significantly improved the tribological performance of the composites. At room temperature (Figure 4(a)), a lubrication film was found to be formed and broken a few times at the interface between the Al₂O₃ ball and Mg MMC disc during testing. The CoF for the two MMCs are close and follow a similar trend over the whole testing period. After the initial increase of CoF in the running in stage, the first formation of the lubricating film lasted around 17 mins where the CoF value was as low as 0.097. Xie et al. [27] reported that the MoS₂ additives, which have the similar crystal structure as WS₂, contributed to the formation and stabilization of the lubricant film in sliding contact between Mg alloy and steel. The friction coefficient was found to be 0.08-0.12 with 1 wt% MoS₂ added in the engine oil. The findings in this study agreed with his conclusion

and confirmed the positive influence of WS₂ in reducing interfacial friction. In addition, under room temperature, the CoF of Mg MMCs did not increase with loads, which indicated an improved load-bearing capacity due to the presence of reinforcements, SiC and WS₂ [43].

Figure 4 (c) and (d) show the influence of temperature on the frictional performance of Mg MMCs and alloy. Sintered pure Mg showed the highest friction coefficient followed by AZ31. Mg MMC1 showed the lowest friction at 110 °C/1 N with an average CoF of 0.15 compared with 0.19 from composite Mg MMC2, shown in Figure 4(c). Ratoi et al. [58] found that in sliding contact, under high pressure and high temperature, WS₂ reacted with the metal substrate and generated a thick chemical tribo-film which accounted for the improved tribological properties of the composites. At 110 °C and P = 4 N, the CoF for pure Mg and AZ31 were slightly decreased due to the thermal softening of the bulk material under high temperature. For both composites, the CoF fluctuated in the running in stage and stabilised after 30 min rubbing. The average CoF was found to be the same, at 0.2 for both Mg composites for the remaining stabilised stage.

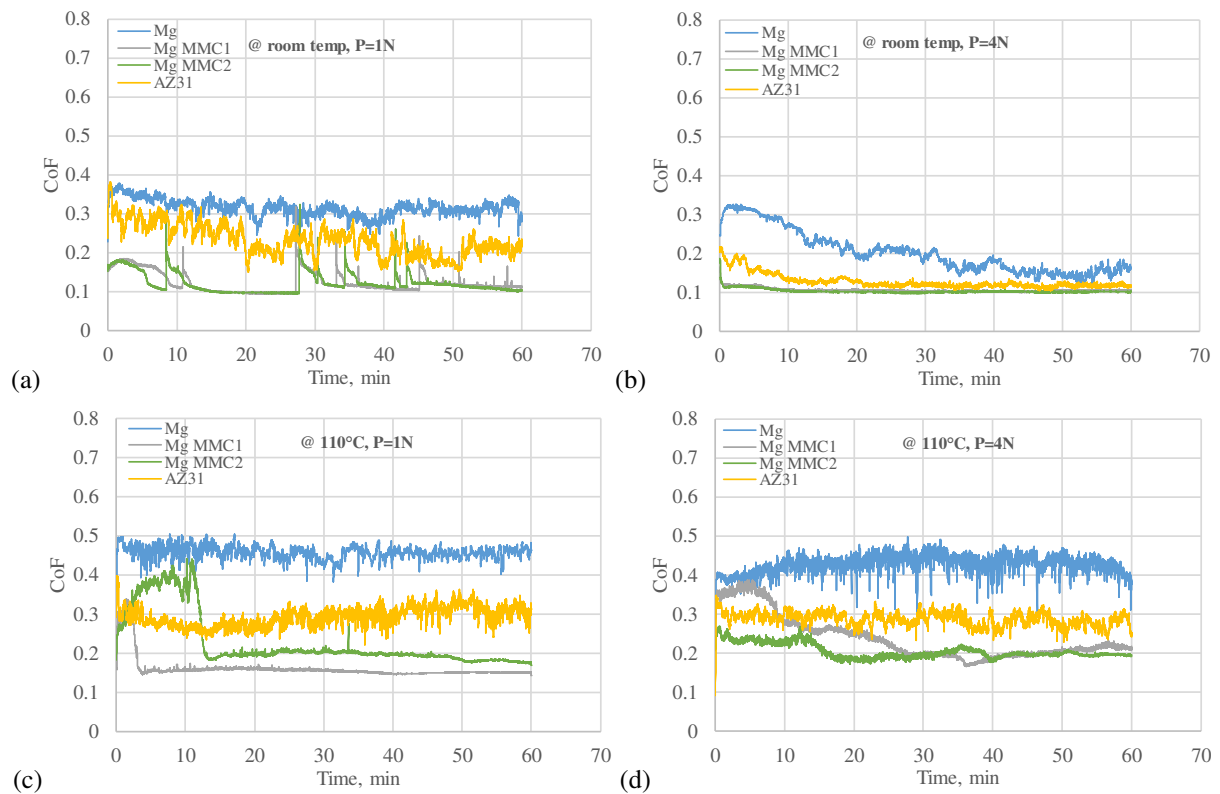


Figure 4. Coefficient of friction varying with reciprocating sliding time for Mg MMCs and Mg alloy, (a) at room temperature, P = 1 N, (b) at 110 °C, P = 1 N, (c) at room temperature, P = 4 N, and (d) at 110 °C, P = 4 N

The CoF difference between the pure Mg, AZ31 and Mg MMCs suggests that the mechanism of friction and lubrication is different in each case and the temperature plays an important role in rubbing. In order to assess the mechanism of the different frictional behaviour and the working mechanism of WS₂ as an effective lubricating additive, characterisations of the disc wear track and the worn ball surface were conducted by using optical microscopy, Alicona profilometry, SEM and EDX.

After each reciprocating sliding test, the discs and ball were cleaned with isopropanol to remove remaining lubricant. The wear tracks on tested discs were assessed using Alicona microscope profilometry to determine the dimensions, including wear volume, wear scar depth and width. SEM microscopic images and EDX mapping were taken for studying the worn

surface morphology and element distribution of the reinforcements. Figure 5 shows a set of the 3D wear track profiles for four tested materials at 110 °C and normal load $P = 4$ N.

From Figure 5 it can be seen that the largest wear track was generated on the Mg disc after 60 min rubbing against alumina ball. The wear depth was found to be 43.42 μm which is approximately 3 times that of Mg MMC1. Mg MMC2 with 20 wt% SiC possessed the best wear resistance of the four materials with a wear scar depth of 10.26 μm . The presence of hard particles of SiC has proven to significantly improve the mechanical strength of the composite. This can also be evidenced by the small contact area on the ball counterface. There was nearly no material transfer observed from the disc onto the ball when contacting with Mg MMCs apart from a small amount of material deposited at the ends of the wear track, shown in Figure 5 (c). Compared with Mg and AZ31, the ball presented a ‘roughened’ worn surface containing wear grooves due to abrasive wear from rubbing against the hard SiC particles on the composite surface. Adhesive wear has been observed on the Mg disc indicated by a transferred layer of Mg oxide on the ball. In addition, the worn zone on the ball was found to be much larger when contacting the Mg disc compared with other materials. This was due to greater deformation on the Mg disc under normal and shear stress. This agreed with the highest wear volume that occurred on the Mg disc, shown in Table 3.

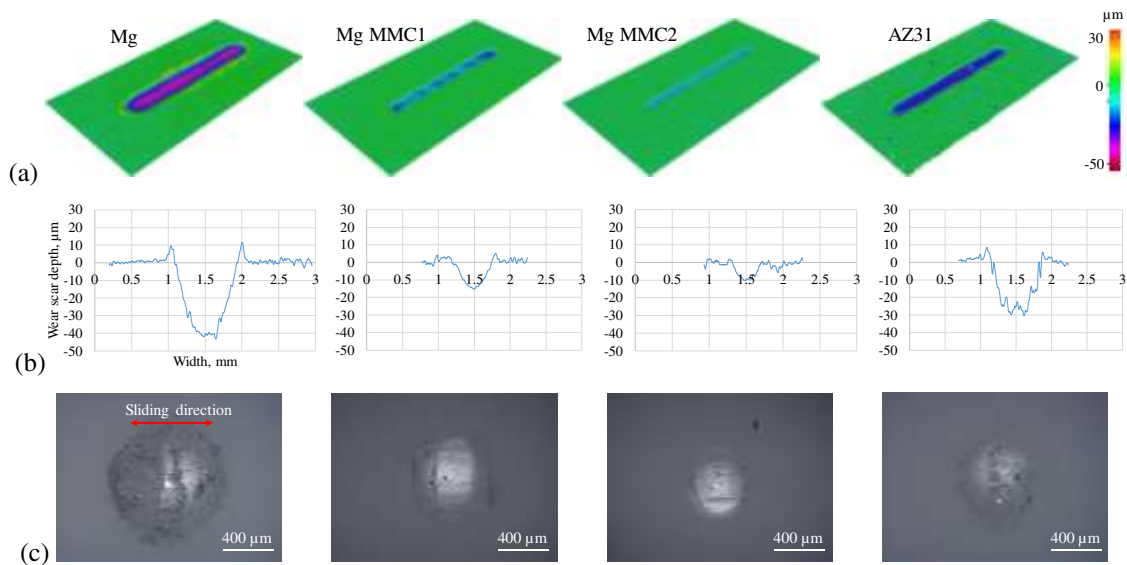


Figure 5. Wear profiles of tested specimens and balls, (a) 3D wear track profile, (b) wear scar depth on tested disc specimens, and (c) wear profile of the counterface on the Al_2O_3 ball at 110 °C, $P = 4$ N

The wear rates W , in $\mu\text{m}^3/\text{Nm}$, were calculated using the following equation,

$$W = \frac{V}{Pvt} \quad (1)$$

Where V is the wear volume, in μm^3 , measured by Alicona, P is the normal load, in N , v is the sliding speed, in m/s and t is the test duration, in s .

Figure 6 shows the wear rate calculated from the wear volume data measured from the Alicona profilometry. In all testing conditions, Mg composites show similar wear resistance which was better than that of pure Mg and Mg alloy. The presence of SiC and WS_2 significantly improved the composite's wear property. At 110 °C and 4 N normal load, Mg MMC2 with higher portion of SiC (20 wt%) has a lower wear rate, $2.03 \times 10^5 \mu\text{m}^3/\text{N/m}$, compared with that of $3.62 \times 10^5 \mu\text{m}^3/\text{N/m}$ for Mg MMC1. Under the same load but room temperature, the wear rate of Mg

MMC2 was $0.78 \times 10^5 \mu\text{m}^3/\text{N}/\text{m}$, which was around 25% of pure Mg and 50% of AZ31. When the load was 1 N, the wear rate wasn't found to increase with temperature for two Mg MMCs. Previous work also reported that, due to the addition of WS_2 in the metal composites, there was a significant reduction of plastic deformation depth at the subsurface leading to lower wear of the bulk material [48].

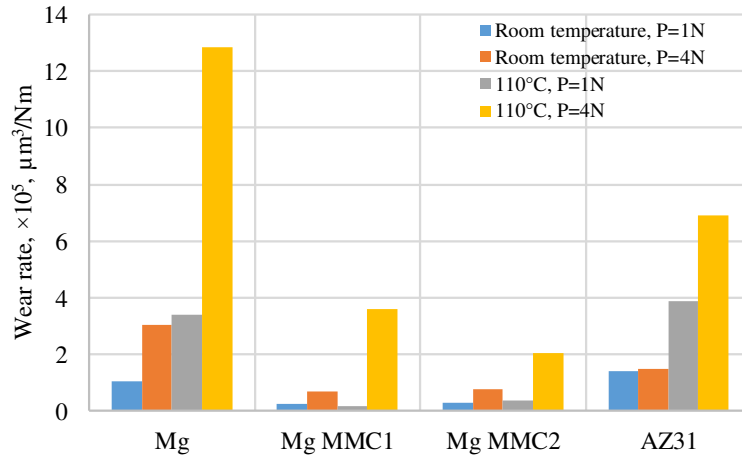


Figure 6. Wear rate of tested materials sliding against Al_2O_3 ball subject to varying testing conditions

Table 4 summarises the wear track dimensions, including wear volume, wear scar depth and width for all tested materials. For all testing conditions, Mg MMCs exhibited excellent anti-wear property. Under the higher testing temperature and normal load, the generated wear scar depths were found to be $15.3 \mu\text{m}$ and $10.26 \mu\text{m}$ for Mg MMC1 and MMC2, which were much smaller than that of unreinforced Mg ($43.42 \mu\text{m}$) and AZ31 ($30.5 \mu\text{m}$).

Table 4. Wear track dimensions and wear rate for tested materials subject to varying testing conditions

		Room temperature			110 °C		
		Max. depth, μm	Width, μm	Wear volume, $\mu\text{m}^3, \times 10^7$	Max. depth, μm	Width, μm	Wear volume, $\mu\text{m}^3, \times 10^7$
Mg	P = 1 N	8.81	440	0.85	15.79	675	2.76
	P = 4 N	18.01	710	2.46	43.42	1050	10.42
Mg MMC1	P = 1 N	2.80	200	0.21	2.10	215	0.14
	P = 4 N	5.11	310	0.55	15.3	620	2.93
Mg MMC2	P = 1 N	5.39	205	0.23	4.38	230	0.31
	P = 4 N	6.45	300	0.63	10.26	480	1.64
AZ31	P = 1 N	8.28	400	1.14	8.90	610	3.13
	P = 4 N	21.18	480	1.21	30.50	760	5.61

In order to study how WS_2 and SiC additive particles improve the anti-wear performance of the Mg composites and determine the predominant wear mechanism on the sliding contact, the wear tracks were investigated using SEM after the friction tests. Figure 7 shows SEM images of the wear tracks for the pure Mg and AZ31 specimens. The wear tracks on the Mg disc appear rougher with larger size wear debris, especially at the higher temperature of $110 \text{ }^\circ\text{C}$ which indicated that seizure and galling occurred on the wear track which was also presented from the contact zone on the counter ball shown in Figure 5. In agreement with the profilometry measurements, the SEM images show greater wear track width on the Mg discs than that on the AZ31 discs.

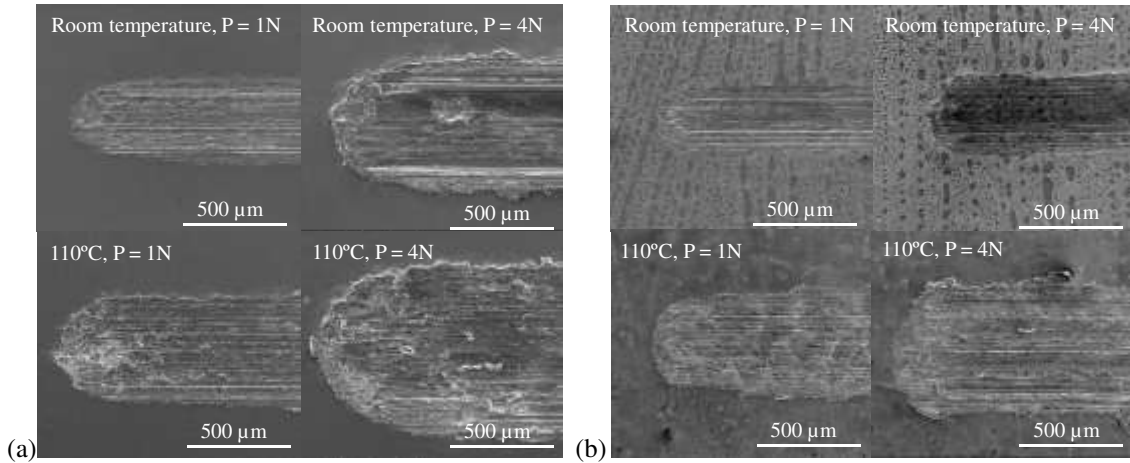
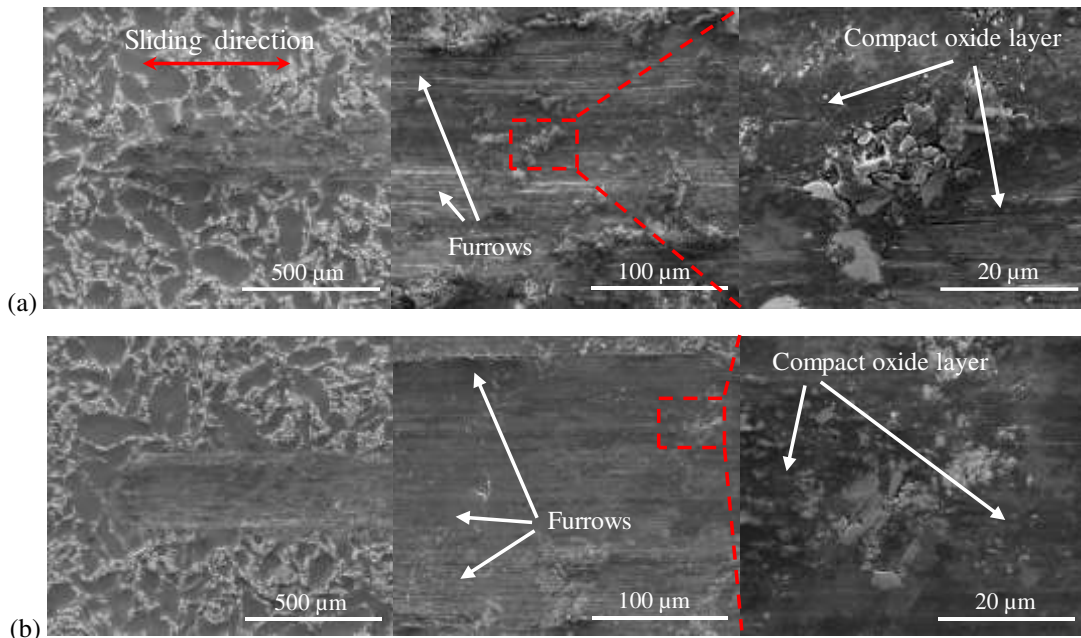


Figure 7. SEM images of wear tracks on the pure Mg and AZ31 specimens tested at room temperature and 110 °C, P = 1,4 N, rubbing against Al₂O₃ ball, (a) Mg and (b) AZ31

Figure 8 shows the SEM images of the wear scar generated on the Mg MMC1 under varying testing conditions. As shown in Figure 8(a) and (b), furrows along the width of the wear track can be observed, indicating that abrasive ploughing dominated the wear mechanism on the tested disc at room temperature. A compact oxide layer probably mixed with WS₂ and some SiC particles was found distributed on the worn surface. On the worn surface from 1 N (Figure 8(a)), Mg particle boundaries can still be observed as indicated by the bright SiC particles. However, higher normal load produced a smoother worn track, barely showing Mg particle boundaries as shown in Figure 8(b). It seems that the hard SiC protrusions were pressed down into the bulk material due to low modulus of the bulk Mg. These embedded SiC particles together with WS₂ particles and Mg oxide formed the tribo-layer that separated the two contacting surfaces of the alumina ball and the Mg matrix composite. The overall morphology of the worn tracks from room temperature tests confirmed the occurrence of mild wear on the Mg matrix.



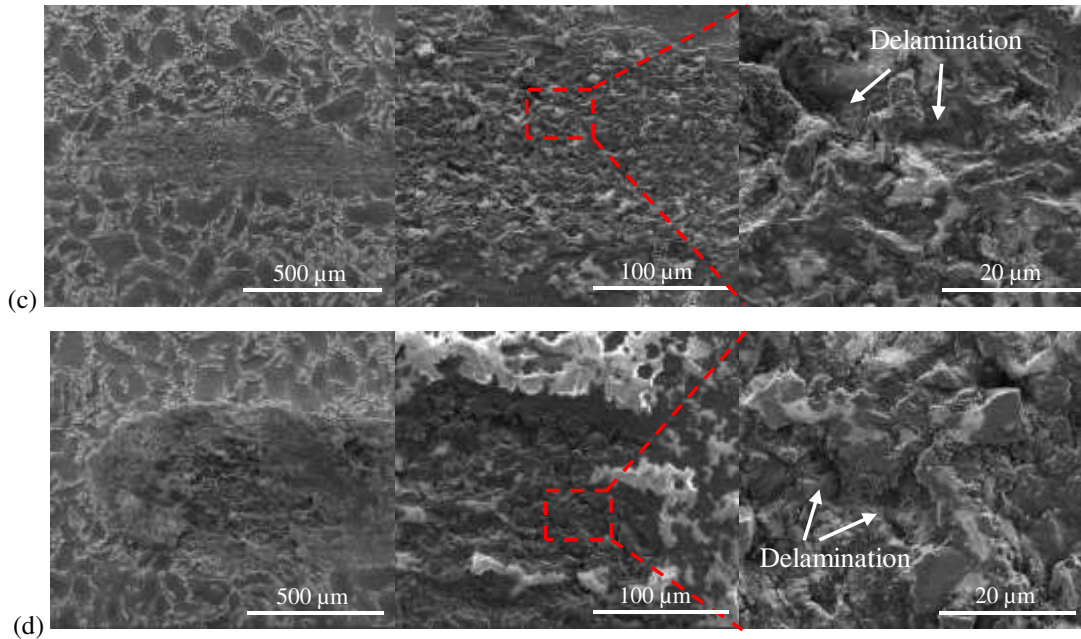


Figure 8. SEM images of the wear tracks on the Mg MMC1 specimen tested at (a) room temperature, $P = 1$ N, (b) room temperature, $P = 4$ N, (c) 110 °C, $P = 1$ N, and (d) 110 °C, $P = 4$ N

The interfacial film, known as tribo-layer in this study, consisting of solid lubricant particles, lubricating oil and wear debris, play an important role in accommodating sliding motion and determining the tribological response of the interface [35, 44]. It is expected that the interaction between oil, reinforcement particles and wear particles at the interface determines essentially the friction and wear behaviour of rubbed surfaces. On one hand, the SiC particles increase the strength of the Mg matrix. On the other hand, the oxides formed under room temperature mixed with WS_2 particles which are spread over the interface due to sliding, act as a protective layer to avoid the transition from abrasion to delamination. Figure 9 shows a sketch of the tribo-layer in the sliding contact. In rubbing, WS_2 particles were flowing with the oil, attached to the composite surface. Microscopic reservoirs were expected to be created by the SiC protrusions. Such reservoirs on the Mg MMC substrate facilitates the retention and recirculation of WS_2 particles in the contact zone between the alumina ball and the metal matrix. Due to the crystal structure of WS_2 sheets, the low shear strength contributes to the reduction of friction [49].

However, the SEM images of the wear tracks from high temperature sliding tests, shown in Figure 8(c) and (d), exhibit severe plastic deformation, which demonstrates adhesive wear on Mg MMC1. Due to the extensive surface deformation, the formation of oxides and furrows caused by abrasive wear cannot be observed on the worn surface, indicating a different wear mechanism when compared with tests at room temperature. This may be due to that the high temperature softening of the substrate and weakening of the bonding between Mg and reinforcement particles, SiC and WS_2 . Due to the shearing and compressing actions, the embedded particles were shifted and redistributed on the substrate surface. This process generated a higher friction coefficient, 0.15, as compared with 0.1 from room temperature at the lower load of 1 N. The wear volume loss at 110 °C was found to be comparable with that at room temperature. This indicated that the redistributed particles together with wear debris still work as a tribo-layer, improving the tribological behaviour of the composite. Under higher load, more severe plastic deformation was expected on the substrate surface and the dominant wear mechanism was considered to be delamination, shown in Figure 8 (d). This indicates that the operating conditions, normal load and temperature, have a great influence in the friction and wear behaviour of the composites. The SEM micrographs agreed with the friction and wear loss values shown in Figure 4 and 6.

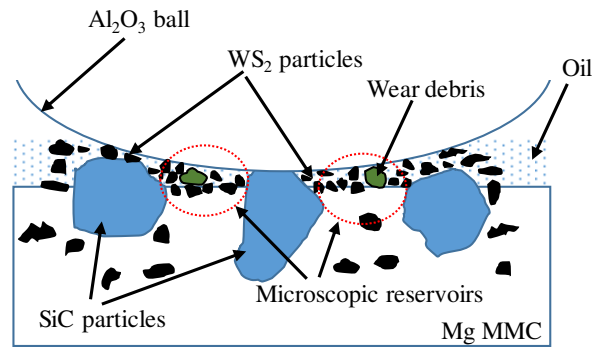


Figure 9. Schematic diagram of the tribo-layer between alumina ball and Mg MMC under sliding friction

In order to explore the working mechanism of the tribo-layer on the worn composite surface, EDX mapping was conducted after the sliding test. As both Mg MMC1 and MMC2 exhibit similar wear resistance, EDX mapping was only conducted on Mg MMC2. Figure 10 shows SEM images of wear tracks on Mg MMC2 with highlighted zones for EDX mapping, detailed in Figures 11-13.

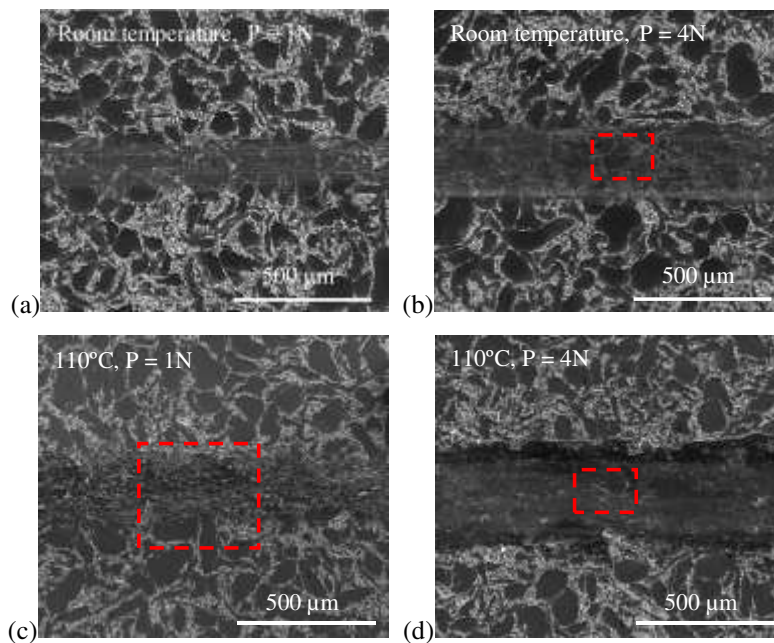


Figure 10. SEM images comparing wear track profiles influenced by testing conditions for Mg MMC2 specimen

Figure 11 (a)-(d) are EDX spectra collected in spot mode from the locations labelled as Spectr 1, 2, and 3 on Figure 11(a), corresponding to the Mg particle, Mg particle boundary and worn track. From Figure 11(b), it can be seen that the Mg peak is the strongest peak which confirms the Mg particle at Spectr 1. At the Mg particle boundary, Spectr 2, apart from Mg peak, W, Si and S also show high intensity corresponding to SiC and WS₂ particles accumulated at Mg particle boundaries, shown in Figure 11(c). Al was detected which indicated the material transfer from the alumina ball, shown in Figure 11(d). Increased intensity of O was detected on the wear track. This is from oxides formed during the sliding friction. The tribo-layer was found to be composed of additive particles, oxides and transferred material from the ball.

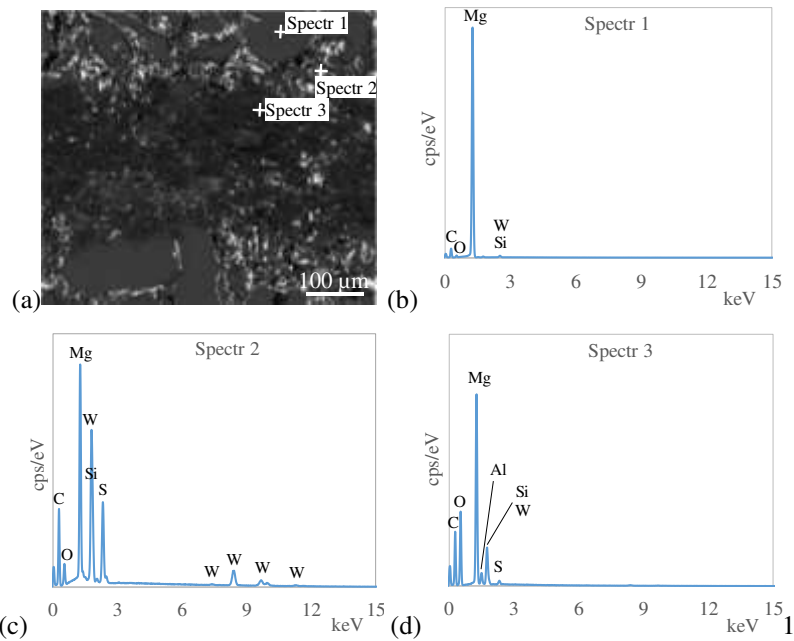
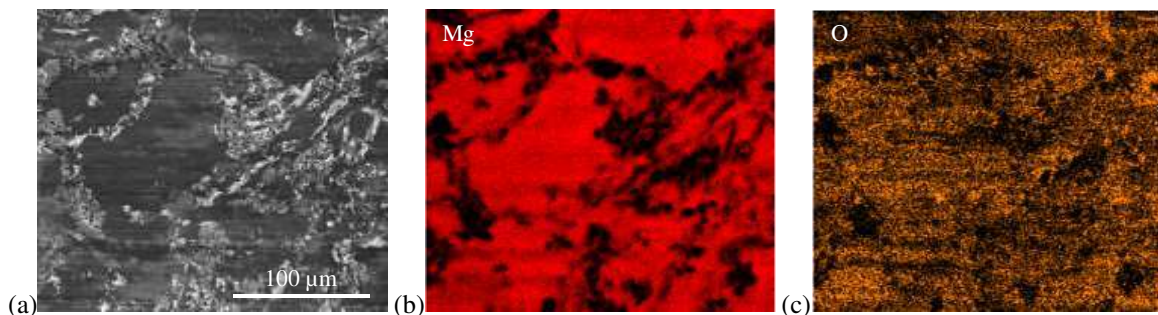


Figure 11. EDX spectrum for the chemical elements distribution from the wear track on Mg MMC2 at 110 °C, P = 1 N, (a) SEM image of the wear track, (b)-(d) EDX spectrum corresponding to locations Spectr 1-3

To get an insight into the composition of the wear track and reveal the wear mechanism, EDX mappings were performed for Mg MMC2 subject to high load and high temperature. Figure 12 shows the mappings corresponding to the worn surface under 4N and room temperature. As it can be seen, the tribo-layer mainly consists of Mg from the matrix, Si, S and W from reinforcements, and oxygen which highly overlapped with Mg indicating that the oxidation reaction has widely taken place on the Mg MMC surface. SiC particles are still found mainly located at the Mg particle boundaries but broken down to smaller sizes due to the high contact pressure and shearing stress, shown in Figure 12(a) and (d). W and S presented a highly consistent distribution pattern shown in Figure 12 (e) and (f). Similar to Si, they are mainly located at the Mg particle boundaries. However, much finer particles containing W and S were found spread over the worn surface. Based on the layer structure of the WS₂ particle, it is reasonable to conclude that micro scaled WS₂ particles have been crushed from flakes into nano-scale particles and spread over the contact zone due to the rubbing motion. These nano-particles contribute to lower friction and wear at the interface.



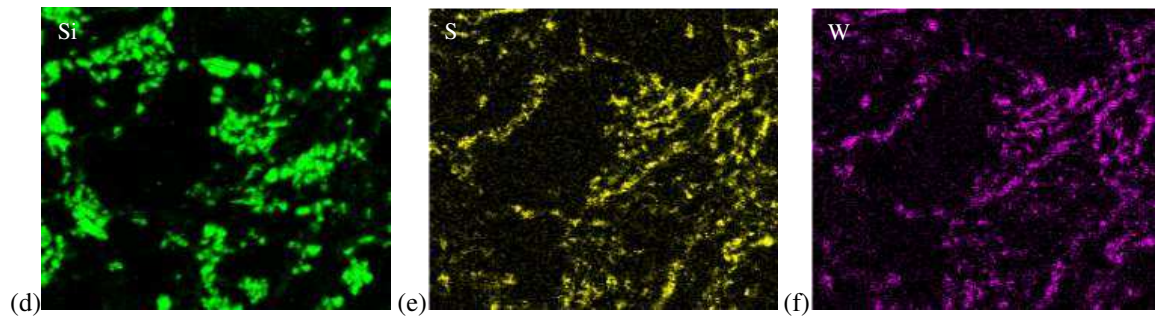


Figure 12. EDX mapping for the chemical element distribution over the Mg MMC2 wear track at room temperature, $P = 4 \text{ N}$, (a) SEM image of the wear track, (b)-(f) chemical elements for Mg, O, Si, S and W

Figure 13 mapped the composition for the worn surface of Mg MMC2 at $110 \text{ }^\circ\text{C}$. From the distribution of Mg, no particle boundaries can be observed, confirming a severe wear mechanism occurred on the surface, shown in Figure 13(b). Si was found to be more evenly distributed on the surface with smaller sized particles. Again, this distribution was thought to be caused by plastic deformation and delamination of the composite. The maps of S and W show an overlapping pattern, indicating the crystal structure of WS_2 did not collapse during sliding. A sweeping redistribution process occurred on WS_2 particles when they were crushed into much finer particles, shown in Figure 13 (e) and (f). Previous studies have shown that chemical reactions may take place between surface, counterface, and the atmosphere. By investigating the interfacial films generated during dry sliding, it was found that tribochemical reactions took place between diamond-like carbon, MoS_2 coatings and Ti implanted steel at the interface when they rub against each other [35]. Niste et al. [43] studied Al metal matrix and found the chemical reaction between WS_2 particles and the metal substrate at temperatures according to the presence of tungsten as WO_3 and W^0 in the tribo-layer. Cao et al. [48] studied the tribological performance of WS_2 reinforced Cu composite through dry sliding tests against a steel ball and found the decomposition of WS_2 while reacting with copper. However, from this study, there was no evidence observed from the EDX mapping that indicated a chemical reaction between WS_2 and the metal substrate. This may due to the role of base oil PAO in sliding, which helped to dissipate the heat from friction.

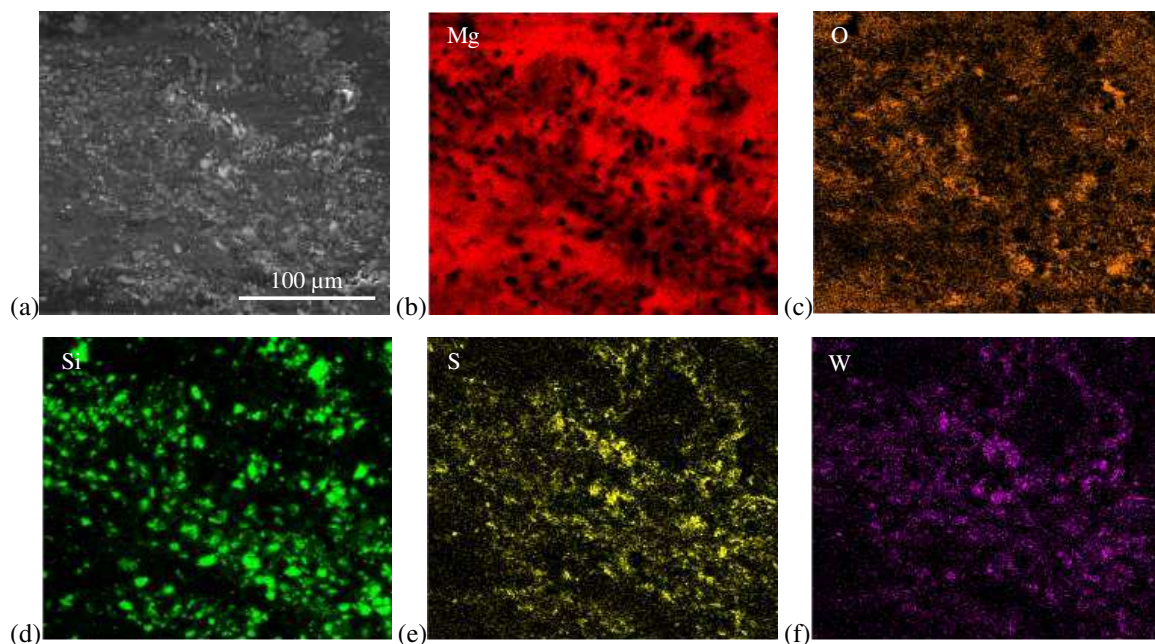


Figure 13. EDX mapping for the chemical elements distribution from the wear track on Mg MMC2 $110 \text{ }^\circ\text{C}$, $P = 4 \text{ N}$, (a) SEM image of the wear track, (b)-(f) chemical elements for Mg, O, Si, S and W

4. Conclusions

Mg based composites reinforced with SiC and WS₂ were designed and successfully sintered through a powder metallurgy technique. The reciprocating sliding tests were conducted using a ball-on-disc configuration under varying normal loads (1-4 N) and testing temperatures (room temperature and 110 °C) against an Al₂O₃ ball lubricated with PAO base oil. From the experimental findings and post-test analysis, conclusions are summarized as:

(1) Compared with unfilled Mg and commercial Mg alloy AZ31, the mechanical properties of the Mg MMCs were markedly enhanced by the SiC particles while the friction and wear properties were improved by WS₂ particles.

(2) During frictional sliding at room temperature, WS₂ spread over the interface and contributed to a tribolayer. Under a normal load of 4 N (~ 0.5 GPa), room temperature and 110 °C, the friction coefficients of Mg MMCs were found to be reduced by 37.5% and 54.5% respectively, along with narrower, shallower and smoother wear tracks, in comparing with unreinforced Mg.

(3) In sliding, WS₂ particles and wear debris were trapped in the microscopic reservoirs created by embedded SiC protrusions on the Mg MMC surface. The findings explain the superior anti-wear behaviour of the WS₂ reinforced Mg composites and are in agreement with studies of lubricating mechanisms of WS₂ additives.

(4) An adhesion wear mechanism on the Mg MMCs occurred under high temperature. For both Mg MMCs, wear was observed on the counter ball under higher contact pressure, ~ 0.5 GPa, which was caused by the abrasive of the SiC particle. Under all testing conditions, the wear resistance of Mg composites was superior to unfilled Mg and Mg alloy.

(5) Mg reinforced with WS₂ and SiC exhibited the outstanding anti-wear and frictional properties in addition to enhanced mechanical strength. This study demonstrates that Mg MMCs provide a competitive advantage to be used as greener components operating in tribological applications.

Acknowledgement

This work was supported by the Aerospace Technology Institute funded project Large Landing Gear of the Future (LLGF) led by Safran Landing Systems [grant number 113077].

The authors gratefully acknowledge Professor W Mark Rainforth for kindly offering the use of Bruker's Universal Mechanical Tester (UMT) platform with REC400 heating chamber. We also thank Dr Righdan Namus for his professional training on the operation of UMT.

Reference

- 1 Canter N. Lightweight self-lubricating metal matrix composites. *Tribology & Lubrication Technology*. 2016; 72:18-19.
- 2 Akinwamide SO, Lemika SM, Obadele BA, Akinribide OJ, Abe BT, Olubambi PA. Characterization and mechanical response of novel Al-(Mg-TiFe-SiC) metal matrix composites developed by stir casting technique. *Journal of Composite Materials*. 2019; 53(28-30):3929-3938.
- 3 Rao G, Vundavilli PR, Saheb KM. Microstructural and mechanical behaviour of Al6061/Gr/WC hybrid metal matrix composite. In: Li L, Pratihari D, Chakrabarty., Mishra P. (eds) *Advances in Materials and Manufacturing Engineering. Lecture Notes in Mechanical Engineering*. Springer, Singapore. 2020.
- 4 Springer H, Baron C, Mostaghimi F, Poveleit J, Mädler L, Uhlenwinkel V. Additive manufacturing of high modulus steels: new possibilities for lightweight design. *Additive Manufacturing*. 2020; In press.

- 5 Valente M, Marini D, Genova V, Quitadamo A, Marra F, Pulci G. Lightweight metallic matrix composites: development of new composites material reinforced with carbon structures. *Journal of Applied Biomaterials & Functional Materials*. 2019; 17(1): suppl.
- 6 Manikandan R, Arjunan TV, Nath AR. Studies on micro structural characteristics, mechanical and tribological behaviours of boron carbide and cow dung ash reinforced aluminium (Al 7075) hybrid metal matrix composite. *Composites Part B: Engineering*. 2020; 183:in press.
- 7 Gupta M, Nai MLS. *Magnesium, magnesium alloys and magnesium composites*. New York: John Wiley & Sons.; 2011.
- 8 Mondal AK, Bhesetti C, Kumar S. Wear behaviour of AE42+20% saffil Mg-MMC. *Tribology International*. 2007; 40: 290-296.
- 9 Thein MA, Lu L, Lai MO. Mechanical properties of nano-structured Mg-5 wt% Al-x wt% AlN composite synthesized from Mg chips. *Composite Structures*. 2006; 75:206-212.
- 10 Shanthi M, Nguyen QB, Gupta M. Sliding wear behaviour of calcium containing AZ31B/ Al₂O₃ nanocomposites. *Wear*. 2010; 269:473-479.
- 11 Cicek B, Ahlatc H, Sun Y. Wear behaviours of Pb added Mg-Al-Si composites reinforced with in situ Mg₂Si particles. *Materials and Design*. 2013; 50:929-935.
- 12 Selvam B, Marimuthu P, Narayanasamy R, Anandkrishnan V, Tun KS, Gupta M, Kamaraj M. Dry sliding wear behaviour of zinc oxide reinforced magnesium matrix nano-composites. *Materials and Design*. 2014; 58:475-481.
- 13 Seenuvasaperumal P, Elayaperumal A, Jayavel R. Influence of calcium hexaboride reinforced magnesium composite for the mechanical and tribological behaviour. *Tribology International*. 2017; 111:18-25.
- 14 Ajith Kumar KK, Pillaia UTS, Pai BC, Chakraborty M. Dry sliding wear behavior of Mg-Si alloys. *Wear*. 2013; 303:56-64.
- 15 Yang ZR, Wang SQ, Zhao YT, Wei MX. Evaluation of wear characteristics of Al₃Tip/Mg composite. *Materials Characterization*. 2010; 61:554-563.
- 16 Lee WB, Lee CY, Kim MK, Yoon J, Kim YJ, Yoen YM, Jung SB. Microstructures and wear property of friction stir welded AZ91 Mg/SiC particle reinforced composite. *Composites Science and Technology*. 2006; 66:1513-1520.
- 17 Blau PJ, Walukas M. Sliding friction and wear of magnesium alloy AZ91D produced by two different methods. *Tribology International*. 2000; 33:573-579.
- 18 Deng KK, Wang CJ, Shi JY, Wu YW, Wu K. Microstructure evolution mechanism of micron particle reinforced magnesium matrix composite at room temperature. *Materials Chemistry and Physics*. 2012; 134:581-584.
- 19 Shen MJ, Wang XJ, Zhang MF, Zhang BH, Zheng MY, Wu K. Microstructure and room temperature tensile properties of 1 μm-SiCp/AZ31B magnesium matrix composite. *Journal of Magnesium and Alloys*. 2015; 3:155-161.
- 20 Landkof B. Development of High Strength Magnesium Based MMC Reinforced with SiC Particles for Satellite Structure Applications. *Materialwissenschaft und Werkstofftechnik*. 2003; 34:395-399.
- 21 Banerjee S, Poria S, Sutradhar G, Sahoo P. Optimization of tribological behavior of Mg-WC nanocomposites at elevated temperature. *International Journal of Surface Engineering and Interdisciplinary Materials Science*. 2020; 8: 25-43.
- 22 Dieringa H. Properties of magnesium alloys reinforced with nanoparticles and carbon nanotubes: a review. *Journal of Materials Science*. 2011; 46:289-306.
- 23 Habibnejad-korayem M, Mahmudi R, Ghasemi HM, Poole WJ. Tribological behaviour of pure Mg and AZ31 magnesium alloy strengthened by Al₂O₃ nanoparticles. *Wear*. 2010; 268:405-412.
- 24 Shanthi M, Lim CYH, Lu L. Effects of grain size on the wear of recycled AZ91 Mg. *Tribology International*. 2007; 40:335-338.
- 25 Nguyen QB, Sim YHM, Gupta M, Lim CYH. Tribology characteristics of magnesium alloy AZ31B and its composites. *Tribology International*. 2015; 82:464-471.
- 26 Fabre A, Masse JE. Friction behavior of laser cladding magnesium alloy against AISI 52100 steel. *Tribology International*. 2012; 46:247-253.
- 27 Xie H, Jiang B, He J, Xia X, Pan F. Lubrication performance of MoS₂ and SiO₂ nanoparticles as lubricant additives in magnesium alloy-steel contacts. *Tribology International*. 2016; 93:63-70.

- 28 Lim CYH, Leo DK, Ang JJS, Gupta M. Wear of magnesium composites reinforced with nano-sized alumina particulates. *Wear*. 2005; 259:620-625.
- 29 Xiao P, Gao Y, Xu F, Yang C, Li Y, Liu Z, Zheng Q. Tribological behavior of in-situ nanosized TiB₂ particles reinforced AZ91 matrix composite. *Tribology International*. 2018; 128:130-139.
- 30 Nie KB, Wang XJ, Wu K, Xu L, Zheng MY, Hu XS. Fabrication of SiC particles-reinforced magnesium matrix composite by ultrasonic vibration. *Journal of Materials Science*. 2012; 47:138-144.
- 31 Abachi P, Masoudi A, Purazrang K. Dry sliding wear behavior of SiCP/QE22 magnesium alloy matrix composites. *Materials Science and Engineering*. 2006; 435-436:653-657.
- 32 Wang XJ, Wu K, Huang WX, Zhang HF, Zheng MY, Peng DL. Study on fracture behavior of particulate reinforced magnesium matrix composite using in situ SE. *Composites Science and Technology*. 2007; 67:2253-2260.
- 33 Prasad SV, McConnell BD. Tribology of aluminium metal-matrix composites: lubrication by graphite. *Wear*. 1991; 149:241-253.
- 34 Rapoport L, Bilik Y, Feldman Y, Homyonfer M, Cohen SR, Tenne R. Hollow nanoparticles of WS₂ as potential solid-state lubricants. *Nature*. 1997; 387:791-793.
- 35 Singer, IL. *Fundamentals of Friction: Macroscopic and Microscopic Processes*. Dordrecht, Netherlands: Kluwer.; 1992.
- 36 Bowden FP, Tabor D. *Friction: An Introduction to Tribology*. New York: Anchor Press; 1973.
- 37 Omrani E, Moghadam AD, Menezes PL, Rohatgi PK. Influences of graphite reinforcement on the tribological properties of self-lubricating aluminum matrix composites for green tribology, sustainability, and energy efficiency-a review. *The International Journal of Advanced Manufacturing Technology*. 2016; 83:325-346.
- 38 Bhushan, B. *Modern tribology handbook, Volume one - Principles of tribology*. Florida: CRC Press Inc.; 2001.
- 39 Rapoport L, Lvovsky M, Lapsker I, Leshinsky V, Volovik Y, Feldman Y, Zak A, Tenne R. Slow release of fullerene-like WS₂ nanoparticles as a superior solid lubrication mechanism in composite matrices. *Advanced Engineering Materials*. 2001; 3:71-75.
- 40 Prasad SV, McDevitt NT, Zabinski JS. Tribology of tungsten disulfide films in humid environments: the role of a tailored metal-matrix composite substrate. *Wear*. 1999; 230:24-34.
- 41 Prasad SV, Zabinski JS, Dyhouse VJ. Pulsed-laser deposition of tungsten disulphide films on aluminium metal-matrix composite substrates. *Journal of materials science letters*. 1992; 11:1282-1284.
- 42 Shi X, Song S, Zhai W, Wang M, Xu Z, Yao J, Din AQU, Zhang Q. Tribological behavior of Ni₃Al matrix self-lubricating composites containing WS₂, Ag and hBN tested from room temperature to 800 °C. *Materials & Design*. 2014; 55:75-84.
- 43 Niste VB, Ratoi M, Tanaka H, Xu F, Zhu Y, Sugimura J. Self-lubricating Al-WS₂ composites for efficient and greener tribological parts. *Scientific Reports*. 2017; 7:14665.
- 44 Rapoport L, Leshchinsky V, Lapsker I, Volovik Y, Nepomnyashchy O, Lvovsky M, Popovitz-Biro P, Feldman, Y, Tenne R. Tribological properties of WS₂ nanoparticles under mixed lubrication. *Wear*. 2003; 255:785-793.
- 45 Al-Samarai RA, Al-Douri Y, Haftirman, Ahmad KR. Tribological properties of WS₂ nanoparticles lubricants on aluminum-silicon alloy and carbon steels, *Walailak Journal of Science and Technology (WJST)*. 2013; 10:277-287.
- 46 Prasad SV, Asthana R. Aluminium metal-matrix composites for automotive applications: tribological considerations. *Tribology Letters*. 2004; 17:445-453.
- 47 Garcia-Lecina E, Garcia-Urrutia I, Diez JA, Fornell J, Pellicer E, Sort J. Codeposition of inorganic fullerene-like WS₂ nanoparticles in an electrodeposited nickel matrix under the influence of ultrasonic agitation. *Electrochimica Acta*. 2013; 114:859-867.
- 48 Cao H, Qian Z, Zhang L, Xiao J, Zhou K. Tribological behavior of Cu matrix composites containing graphite and tungsten disulfide. *Tribology Transactions*. 2014; 57:1037-1043.
- 49 Niste VB, Ratoi M. Tungsten dichalcogenide lubricant nanoadditives for demanding applications. *Materials Today Communications*. 2016; 8:1-11.
- 50 Ratoi M, Niste VB, Zekonyte J. WS₂ nanoparticles-potential replacement for ZDDP and friction modifier additives. *RSC Advances*. 2014; 4:21238-21245.

- 51 Prasad SV, Zabinski JS. Tribology of tungsten disulphide (WS_2): characterization of wear-induced transfer films. *Journal of Materials Science Letters*. 1993; 12:1413-1415.
- 52 Prasad SV, Mecklenburg KR. Self-lubricating aluminum metal-matrix composites. US Patent 5534044. 1996.
- 53 Muhammad WNAW, Sajuri Z, Mutoh Y, Miyashita Y. Microstructure and mechanical properties of magnesium composites prepared by spark plasma sintering technology. *Journal of Alloys and Compounds*. 2011; 509:6021-6029.
- 54 Guan D, Rainforth WM, Sharp J, Gao J, Todd I. On the use of cryomilling and spark plasma sintering to achieve highstrength in a magnesium alloy. *Journal of Alloys and Compounds*. 2016; 688:1141-1150.
- 55 Guan D, Gao J, Sharp J, Rainforth M. Enhancing ductility and strength of nanostructured Mg alloy by in-situ powder casting during spark plasma sintering. *Journal of Alloys and Compounds*. 2018; 769:71-77.
- 56 Pharr GM, Oliver WC, Brotzen FR. On the generality of the relationship among contact stiffness, contact area, and elastic-modulus during indentation. *Journal of Materials Research*. 1992; 7:613-617.
- 57 Oliver WC, Pharr GM. An improved technique for determining hardness and elastic modulus using load and displacement sensing indentation experiments. *Journal of Materials Research*. 1992; 7:1564-1583.
- 58 Ratoi M, Niste VB, Zekonyte J. Mechanism of action of WS_2 lubricant nanoadditives in high-pressure contacts. *Tribology Letters*. 2013; 52:81-91.